An X-ray Diffraction Investigation of Corneal Structure in Lumican-Deficient Mice

Andrew J. Quantock,[1] *Keith M. Meek,*[1] *and Shukti Chakravarti* [2,3]

Purpose. The corneas of mice homozygous for a null mutation in lumican, a keratan sulfate–containing proteoglycan, are not as clear as normal. In the present study, mutant corneas were examined by synchrotron x-ray diffraction to see what structural changes might lie behind the loss of transparency.

Methods. X-ray diffraction patterns were obtained from the corneas of 6-month-old and 2-month-old lumican-null and wild-type mice. Measured in each cornea were the average collagen fibril diameter, average collagen fibril spacing, and the level of order in the collagen array.

Results. The x-ray reflection arising from regularly packed collagen was well-defined on all x-ray patterns from 6-month-old wild-type corneas. Patterns from 6-month-old lumican-deficient corneas, however, contained interfibrillar reflections that were measurably more diffuse, a fact that points to a widespread alteration in the way the collagen fibrils are configured. The same distinction between mutant and wild-type corneas was also noted at 2-months of age. Average collagen fibril spacing was marginally higher in corneas of 6-month-old lumican-null mice than in corneas of normal animals. Unlike x-ray patterns from wild-type corneas, patterns from lumican-deficient corneas of both ages registered no measurable subsidiary x-ray reflection, evidence of a wider than normal range of fibril diameters.

Conclusions. The spatial arrangement of stromal collagen in the corneas of lumican-deficient mice is in disarray. There is also a considerable variation in the diameter of the hydrated collagen fibrils. These abnormalities, seen at 2 months as well as 6 months of age, probably contribute to the reduced transparency. (*Invest Ophthalmol Vis Sci.* 2001;42:1750–1756)

It has long been supposed that negatively charged glycosaminoglycans in the cornea have a bearing on the tissue's clarity. For example, it is known that the most abundant corneal glycosaminoglycan, keratan sulfate, is undersulfated in opaque corneal scars in adult rabbits.[1–4] Moreover, the developing chick cornea synthesizes a lactosaminoglycan (i.e., unsulfated) form of keratan sulfate in the early stages of development when it is opaque, to be followed by a sulfated glycosaminoglycan form some days later when it becomes transparent.[5–7] Also, in newborn mice, keratan sulfate core proteins are abundant in the cornea by postnatal day 10, whereas sulfated keratan sulfate proteoglycans are only detected after the eyes open, leading some investigators to suggest a contribution to corneal transparency.[8] In humans, too, sulfated keratan sulfate is thought to be functionally important, because it is this molecule that is missing in the most common forms of macular corneal dystrophy,[9–10] a disease in which corneal opacification is usually treated by keratoplasty.

In the cornea, three types of small proteoglycan have been identified that contain keratan sulfate side chains: lumican,[11] keratocan,[12,13] and mimecan (or osteoglycin).[14] Recently, work at the genetic level has directly demonstrated the importance of lumican in corneal transparency when it was shown that mice homozygous for a null mutation in this molecule have opaque corneas.[15,16] In these animals, a bilateral corneal opacity is usually detectable by slit lamp examination anywhere from 6 weeks to 5 months and is generally diffuse and confined to the central cornea with a peripheral clear zone. In vivo confocal microscopy has disclosed increased backscattering (an indication of loss of transparency) in the corneas of the null mice as early as 3 to 4 weeks of age.[17] We have not detected progression of these opacities in follow-up studies.

It is believed that keratan sulfate in the cornea helps (along with other corneal glycosaminoglycans) to maintain collagen fibrils in a specific spatial conformation.[18] This arrangement of fibrils, in turn, is understood to be a significant contributory factor to the cornea's light transmission properties.[19–22] The corollary is that a breakdown of the normal stromal architecture, if it is severe enough, leads to increased light scattering and hence to corneal cloudiness. Indeed, an electron microscopic inspection of the corneas of lumican-deficient mice has indicated the presence of structural collagen abnormalities in localized regions of the tissue that might well be to the detriment of tissue transparency.[17]

To investigate the ultrastructure of the corneas of lumican-null mice, we undertook a series of experiments using synchrotron x-ray diffraction, a technique that directs a focused beam of monochromatic x-rays through the whole thickness of the cornea, and in doing so provides average values for regularly occurring spatial elements in the whole volume of the tissue through which the beam, ordinarily a few millimeters in size, passes.[23] In recent years, a substantial amount of new data has been gained by x-ray diffraction experiments in the cornea.[24–29] This is because, as well as providing structural information from an immense number of scattering elements (i.e., collagen fibrils), the approach has the added advantage that corneas can be studied at close to physiologic hydration. Thus, dehydration- and fixation-induced artifacts, unavoidable in electron microscopy,[30] are not a major issue.

Methods

Animals

Gene-targeted mice, homozygous for a null mutation in lumican (lum^{tm1sc}/lum^{tm1sc}),[15,17] were bred and housed in a pathogen-free

From the [1]Biophysics Group, Department of Optometry and Vision Sciences, Cardiff University, United Kingdom; and the [2]Departments of Medicine, Genetics and Ophthalmology, Case Western Reserve University, Cleveland, Ohio.

[3]Present affiliation: Departments of Medicine, Cell Biology and Ophthalmology, Johns Hopkins University, Baltimore, Maryland.

Presented at the annual meeting of the Association for Research in Vision and Ophthalmology, Fort Lauderdale, Florida, May 2000.

Supported by Grant EY11654-03 from the National Institutes of Health, the BBSRC, Daresbury Lab CLRC, and a programme grant from the Medical Research Council, United Kingdom.

Submitted for publication December 13, 2000; revised March 2, 2001; accepted March 21, 2001.

Commercial relationships policy: N.

The publication costs of this article were defrayed in part by page charge payment. This article must therefore be marked "*advertisement*" in accordance with 18 U.S.C. §1734 solely to indicate this fact.

Corresponding author: Andrew J. Quantock, Biophysics Group, Department of Optometry and Vision Sciences, Cardiff University, Redwood Building, King Edward VII Avenue, Cathays Park, Cardiff CF10 3NB, UK. quantockaj@cf.ac.uk

facility at Case Western Reserve University (Cleveland, OH). At all times the ARVO Statement for the Use of Animals in Ophthalmic and Vision Research was adhered to. Twenty-four corneas were used in these experiments. At prescribed times animals were killed and their corneas immediately excised. One set of 12 corneas, comprising six mutant corneas (four 6-month-old and two 2-month-old) and six wild-type (*lum*$^+$/*lum*$^+$) corneas (again, four 6-month-old and two 2-month-old), was plunged in liquid nitrogen, wrapped in plastic film to limit evaporation, and stored frozen. To help ensure that any structural changes in the corneas were unlikely to be a result of freezing, an identical group of 12 corneas was immersed and stored in glutaraldehyde before x-ray examination. Specimens were then shipped to Cardiff University, either in fixative at ambient temperature or frozen in dry ice.

Synchrotron X-ray Diffraction

Corneas, secured in airtight specimen holders between two sheets of polyester film, were analyzed at the Synchrotron Radiation Source (SRS), Daresbury Laboratory (Cheshire, UK). Each specimen was placed in the path of a focused (1.5 × 1.0 mm), monochromatic (λ = 0.154 nm) x-ray beam on SRS Station 2.1 and the shutters opened to expose the cornea for 10 minutes. In this manner we were able to record low-angle x-ray diffraction patterns for all specimens on a multiwire, gas proportional-area detector situated directly behind the cornea, 8.5 m away. An evacuated tube with polyester film windows separated the specimen from the detector, and the window nearest the detector contained a lead backstop positioned to stop the x-ray beam that passed through the cornea undeviated.

X-ray patterns (512 × 512 pixels) were analyzed with purpose-written, Unix-based software followed by a graphics and statistics package (Statistica; Statsoft, Tulsa, OK). First, x-ray patterns were normalized using ion chamber counts to account for beam intensity decay. A detector response from a 2.5-hour exposure to a radioactive source (Fe^{55}) was then subtracted from each x-ray pattern to correct for any nonlinearities in the detector. Next, a vertical scan, 28 pixels wide, of x-ray intensity (I) versus radial position (R) was taken across the center of the pattern. From this, the intensity profile of the first-order equatorial x-ray reflection was readily visible. The intensity profile was then summed about its center, and a plot of R versus $I \cdot R$ generated to correct for the fact that the scan across the circular x-ray pattern was linear. A background representing diffuse x-ray scatter was then fitted to the intensity scans (a power law in the form $y = a + b \cdot x^c$ was found to be suitable) and subtracted from the pattern to leave peaks corresponding to the low-angle x-ray reflections from the cornea.

As is described in detail elsewhere,[23] the equatorial portion of the low-angle x-ray scattering pattern from the cornea is given by

$$I(\boldsymbol{K}) = F^2 \cdot G(\boldsymbol{K})$$

where F^2 is the scattered intensity for a single cylinder (i.e., collagen fibril), and $G(\boldsymbol{K})$ is the interference function. $G(\boldsymbol{K})$ depends on the relative positions of the cylinders and on the scattering vector $\boldsymbol{K}$, and measuring the position of the first maximum of this function—that is, the position of the first-order equatorial reflection—provides a value for the mean center-to-center collagen fibril Bragg spacing. It is for this reason that in cornea the first-order equatorial reflection is often referred to as the interfibrillar reflection. In these experiments, as is usual, the camera was calibrated using the sharp meridional x-ray reflections from rat tail tendon—reflections that index on 67 nm. To convert the interfibrillar Bragg spacings to actual interfibrillar spacings one would have to take packing into account and generally a multiplication factor of 1.12, representative of liquidlike packing is used.[31]

As well as providing a measure of collagen fibril separation, the interfibrillar reflection also provides an estimate of the degree of local order in the arrangement of the collagen matrix. The sharper the reflection (i.e., the narrower the peak in the x-ray intensity scan), the narrower the range of nearest-neighbor spacings and vice versa. The quantity used in this study to represent this is the ratio of peak height to peak width at half height.

In cornea, the scattered amplitude (F) is commonly called the fibril transform, and gives a measure of the average size of the collagen fibrils that contribute to the diffraction pattern. If, like Worthington and Inouye,[31] we assume that the interference function is essentially constant after the innermost maximum and that subsidiary x-ray intensity maxima arise solely from the fibril transform, we can use the reciprocal space positions (Q_n) of the subsidiary maxima to calculate the average collagen fibril diameter (D) from

$$D = 5.14/\pi Q_1 \text{ and } D = 8.42/\pi Q_2$$

where $n = 1$ is the first subsidiary intensity maximum and $n = 2$ the second, and where the numerical factors derive from Bessel functions.[32] The position of either or both subsidiary maxima can be used to obtain a value for the average diameter of the collagen fibrils,[33] and in these studies we used the first—that is, $n = 1$.

Results

X-ray diffraction patterns from the 6-month-old wild-type corneas that had been stored frozen were typical of low-angle patterns from mature cornea, in that a broad but well-defined first-order equatorial x-ray reflection was readily visible. This was true of all four 6-month-old *lum*$^+$/*lum*$^+$ corneas stored in this manner—a fact that was confirmed by the presence on the vertical intensity scans across the centers of the x-ray patterns of two easily recognizable peaks (representing either side of

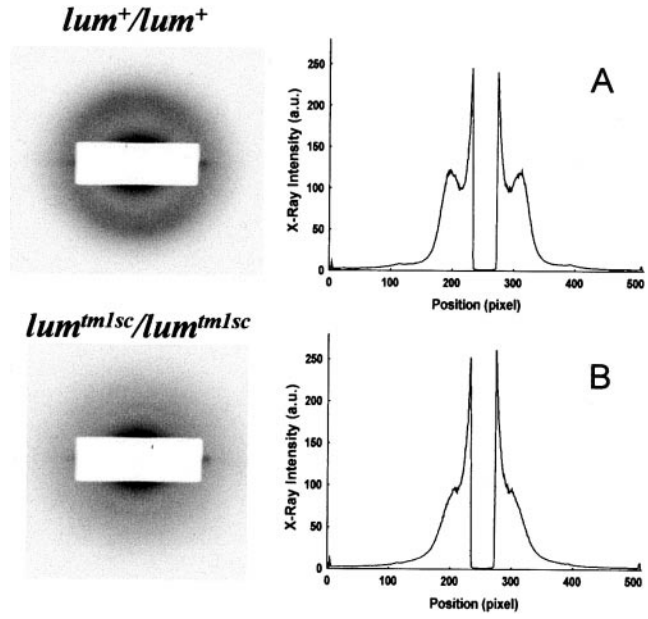

Figure 1. Low-angle x-ray diffraction patterns from a 6-month-old normal (*lum*$^+$/*lum*$^+$) mouse cornea (cornea A; Table 1) and the cornea of a lumican-null (*lum*^{tm1sc}/*lum*^{tm1sc}) mouse of the same age (cornea E, Table 1). Both had been stored frozen. The central white rectangle is the shadow of the lead backstop, which stops the straight-through x-ray beam, and the patterns are typical of all other specimens. A circular interfibrillar reflection is visible on the x-ray pattern from the *lum*$^+$/*lum*$^+$ cornea, but not on the pattern from the *lum*^{tm1sc}/*lum*^{tm1sc} cornea. A vertical x-ray intensity scan (arbitrary units) through the center of this wild-type diffraction pattern (**A**) confirmed the presence of a well-defined interfibrillar reflection. The intensity scan across the lumican-null cornea (**B**) did not provide a well-defined interfibrillar reflection, although some x-ray scattering due to fibrillar organization was noted.

the x-ray reflection; Fig. 1). In marked contrast, all low-angle x-ray scattering patterns from the 6-month-old *lum*^{tm1sc}/*lum*^{tm1sc} corneas that had been stored frozen had no distinct first-order equatorial reflection (Fig. 1). In these cases, however, the vertical intensity scans, which are better able to indicate small changes in x-ray intensity, provided some indication of marginally increased x-ray scattering above background in the region of the first-order equatorial reflection (Fig. 1).

X-ray patterns, similarly obtained, from the 6-month-old *lum*^{tm1sc}/*lum*^{tm1sc} and *lum*$^{+}$/*lum*$^{+}$ corneas that had been stored in fixative revealed the same effect: The interfibrillar reflections from the mutant corneas were much less well-defined than those from the wild-type corneas. Indeed, because fixation itself caused the interfibrillar reflection from the wild-type corneas to diminish, the corresponding reflection from the mutant corneas was not detectable at all (data not shown). Thus, first-order equatorial x-ray reflections produced by the corneas of normal 6-month-old mice and by the corneas of lumican-null mice of the same age were shown to be manifestly different, both when the corneas were stored frozen and when they were stored in fixative. Given that these reflections are formed by regularly spaced collagen fibrils in the corneal stroma, a breakdown of the normal fibrillar ultrastructure is indicated.

X-ray scattering patterns from the mutant and wild-type corneas that had been stored frozen contained better quality data than those that had been stored in fixative. Patterns from the cryopreserved corneas were therefore further analyzed to provide average measurements of corneal ultrastructure. When these x-ray intensity profiles were summed around their centers (Fig. 2), it was recognized that the interfibrillar reflections were invariably much broader in patterns from 6-month-old *lum*^{tm1sc}/*lum*^{tm1sc} corneas than from 6-month-old wild-type corneas. As previously,[34] we quantified the sharpness of the reflection by measuring the ratio of peak height to peak width at half height (after the subtraction of background scatter). Higher ratios are evidence of more local order in the collagen matrix, and it was discovered that the ratio for the 6-month-old wild-type cor-

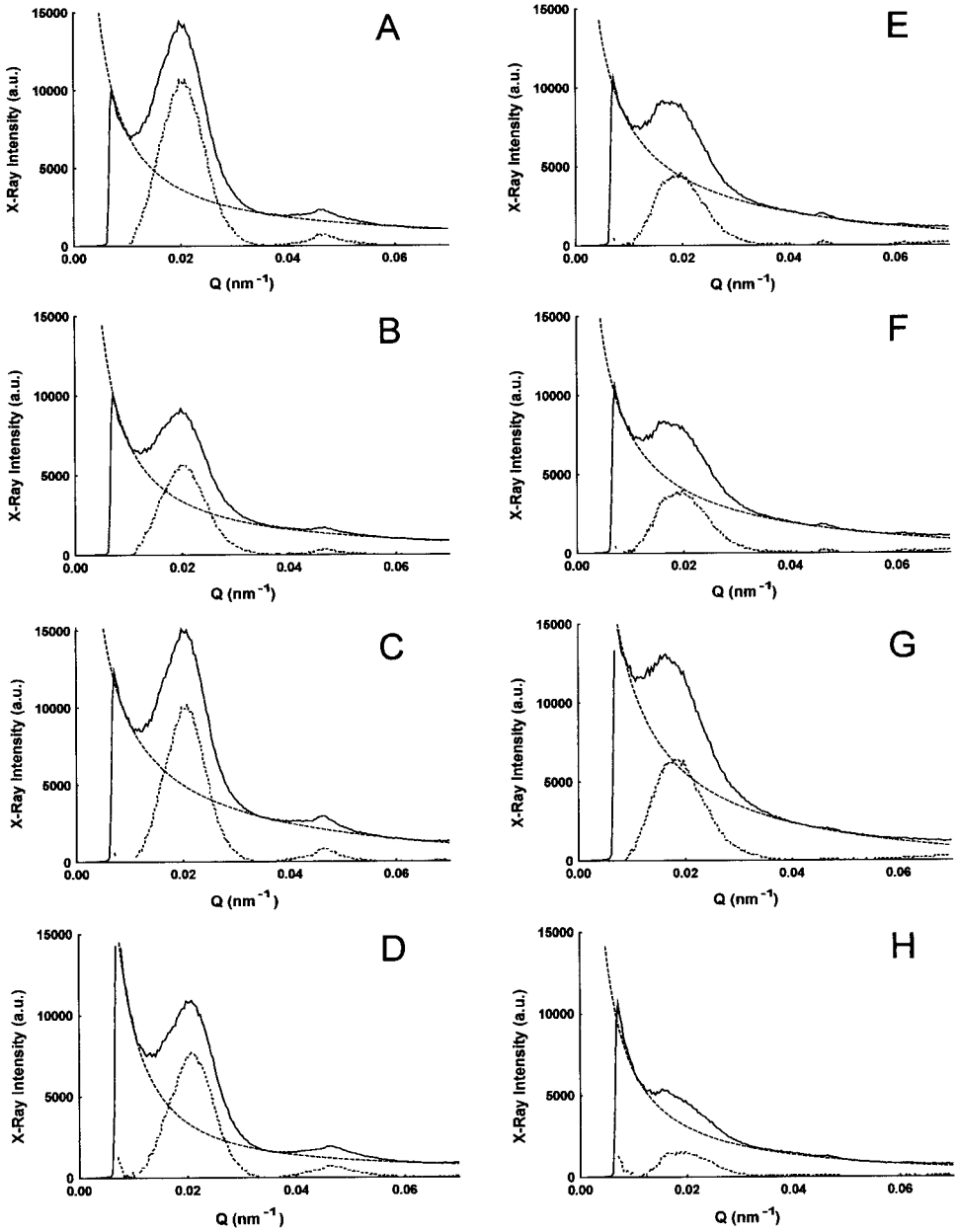

FIGURE 2. X-ray intensity profiles through the centers of the diffraction patterns from the 6-month-old wild-type (**A**–**D**) and 6-month-old lumican-null corneas (**E**–**H**) that had been stored frozen. The two sides of the symmetrical pattern (as seen in Fig. 1) were summed around its center and the system calibrated with a diffraction pattern from rat tail tendon to plot x-ray intensity against reciprocal space distance: Q (in nanometers^{-1}). A background (*dashed line*) subtracted from the raw data (*solid line*) provided a background-subtracted intensity scan (*dotted line*) that enabled measurement of the position of the interfibrillar peak, as well as an indication of its sharpness. In (**A**) through (**D**) an increase in x-ray intensity in the region of $Q = 0.045$ nm^{-1} is due to a subsidiary x-ray reflection (the fibril transform) that gives a measure of the average diameter of collagen fibrils in the corneas. This reflection is not seen in traces (**E**) through (**H**) from the *lum*^{tm1sc}/*lum*^{tm1sc} corneas. a.u.: Arbitrary units.

TABLE 1. Ratio of Peak Height to Peak Width at Half Height, the Average Collagen Interfibrillar Bragg Spacing, and the Average Collagen Fibril Diameter for the Corneas of 6-Month-Old Wild-Type (lum^{+}/lum^{+}) and Lumican-Deficient (lum^{tmlsc}/lum^{tmlsc}) Mice

Cornea	Status	Ratio	Interfibrillar Bragg Spacing (nm)	Fibril Diameter (nm)
A	lum^{+}/lum^{+}	363	49.2 ± 0.4	35.4 ± 0.3
B	lum^{+}/lum^{+}	196	49.6 ± 0.4	34.9 ± 0.3
C	lum^{+}/lum^{+}	369	48.8 ± 0.4	35.4 ± 0.3
D	lum^{+}/lum^{+}	277	48.0 ± 0.4	35.2 ± 0.3
E	lum^{tmlsc}/lum^{tmlsc}	146	52.2 ± 1.0	—
F	lum^{tmlsc}/lum^{tmlsc}	115	51.3 ± 1.0	—
G	lum^{tmlsc}/lum^{tmlsc}	188	55.0 ± 1.0	—
H	lum^{tmlsc}/lum^{tmlsc}	49	51.3 ± 1.0	—

neas was at least double that for the 6-month-old mutant corneas (Table 1).

From the positions of the interfibrillar reflections we discovered that the center-to-center collagen fibril spacing, as an average throughout the whole thickness of the tissue, was consistently, but only marginally, higher (by approximately 7%) in the corneas of 6-month-old mutants than it was in the corneas of 6-month-old wild-types (Table 1). The background-subtracted x-ray scans also revealed that a subsidiary maximum (the fibril transform) was present on all x-ray intensity scans from the 6-month-old lum^{+}/lum^{+} corneas that had been stored frozen (Fig. 2). From the positions of these maxima we were able to calculate the average diameter (*D*) of the collagen fibrils that gave rise to the x-ray scatter (Table 1). These are not appreciably different from normal. An important finding of this study was that no clear and consistently measurable subsidiary maxima were detected in any of the x-ray patterns from the corneas of 6-month-old lum^{tm1sc}/lum^{tm1sc} mice (Fig. 2). This is significant, because it is consistent with the fact that, on average, throughout the whole cornea, the mutant corneas contained a population of collagen fibrils that were not as uniform in size as were the fibrils in normal murine cornea.

To determine whether the structural aberrations in the corneas of 6-month-old lumican-deficient mice might be a function of age, we similarly examined the corneas of 2-month-old animals. The data from the corneas that had been stored frozen (the tissues from which the better-quality x-ray data were obtainable) are shown in Figure 3, and reveal that structural differences in the corneas of the younger mice tended to mirror those of their older counterparts. The interfibrillar spacings in the corneas of 2-month-old lumican-deficient mice were virtually identical with those of the older mutants, as was the interfibrillar spacing in one of the two wild-type corneas (Table 2). Of particular importance, as in the 6-month-old corneas, the ratio of peak height to peak width at half height of the interfibrillar reflection for the 2-month-old lum^{tm1sc}/lum^{tm1sc} corneas was at least double that for the 2-month-old lum^{+}/lum^{+} corneas, pointing to more fibrillar disorder in the mutant tissue. Also, the first subsidiary maximum of the fibril transform—a reflection that showed the average collagen fibril diameter in the corneas of the 2-month-old wild-type mice, similar to that of the 6-month-old wild-type mice, to be approximately 35 nm (Table 2)—was greatly diminished in x-ray patterns from 2-month-old mutant corneas. Again, this is consistent with the fact that, on average, throughout the whole thickness of the tissue, the diameter of the corneal collagen fibrils in mice was less uniform when lumican was not present.

TABLE 2. Ratio of Peak Height to Peak Width at Half Height, the Average Collagen Interfibrillar Bragg Spacing, and the Average Collagen Fibril Diameter for the Corneas of 2-Month-Old Wild-Type (lum^{+}/lum^{+}) and Lumican-Deficient (lum^{tmlsc}/lum^{tmlsc}) Mice

Cornea	Status	Ratio	Interfibrillar Bragg Spacing (nm)	Fibril Diameter (nm)
A	lum^{+}/lum^{+}	256	49.2 ± 0.4	35.1 ± 0.3
B	lum^{+}/lum^{+}	450	56.0 ± 0.4	35.4 ± 0.3
C	lum^{tmlsc}/lum^{tmlsc}	180	51.3 ± 1.0	—
D	lum^{tmlsc}/lum^{tmlsc}	93	51.3 ± 1.0	—

DISCUSSION

It was immediately evident from our studies that the x-ray reflections arising from the regularly packed collagen fibrils in the 6-month-old lumican-null corneas were substantially more

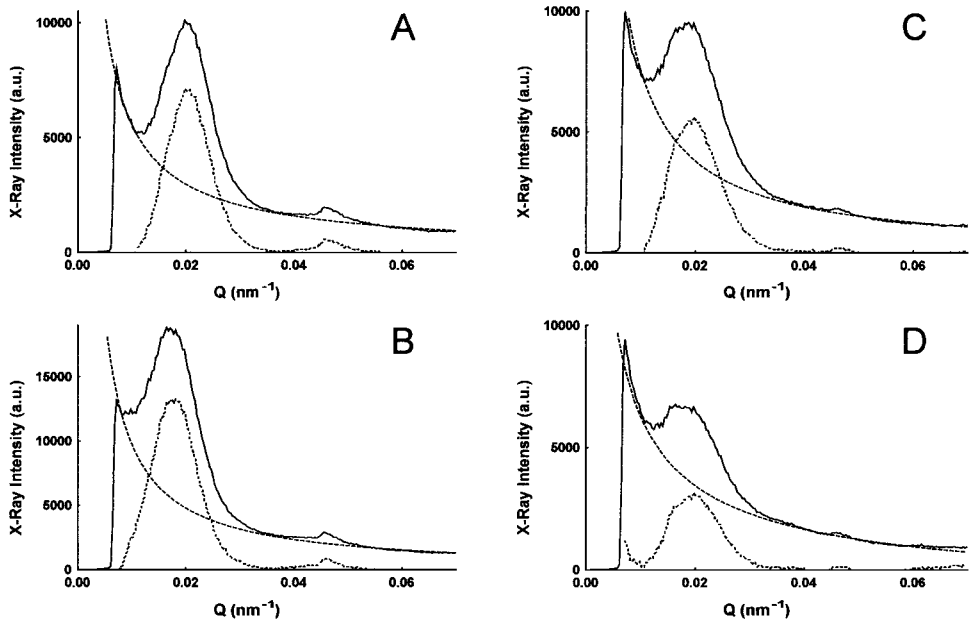

FIGURE 3. X-ray intensity profiles through the centers of the diffraction patterns from the 2-month-old wild type (**A**, **B**) and 2-month-old lumican-null corneas (**C**, **D**) that had been stored frozen. For explanation of the data, see Figure 2.

diffuse than the corresponding reflections from normal murine corneas of the same age. This was true of tissues that had been stored frozen and of those that had been chemically fixed. However, because fixation itself diminished the sharpness of the diffraction patterns, the frozen data were the more useful for structural measurements, and it is this that is shown in Figures 1, 2 and 3. (Chemical fixation for electron microscopy is known to cause some shrinkage in corneal tissue.[30] It now appears that it also induces some alteration in the arrangement of the collagen fibrils, something that we intend to investigate further). The diffuseness of the interfibrillar x-ray reflections from the lum^{tm1sc}/lum^{tm1sc} corneas was confirmed by the fact that the ratio of the height of each interfibrillar reflection to its width at half height on each intensity scan was less than half the ratio in the lum^{+}/lum^{+} corneas (Table 1). As is outlined in more detail elsewhere,[23] a perfect lattice of scattering centers (in this case, collagen fibrils) gives rise to true diffraction maxima, similar to those from a crystal, that appear as very sharp peaks on an x-ray intensity scan. Totally amorphous structures, on the other hand, give rise only to diffuse x-ray scatter. Structures part way between these two extremes form interference maxima whose sharpness is a function of the level of local order in the tissue. The sharper the peak, the narrower the range of nearest-neighbor distances between the scatterers and vice versa. Thus, on average, throughout the whole thickness of the tissue, the configuration of collagen fibrils in the 6-month-old lumican-null corneas was demonstrably less well ordered than the array of collagen fibrils in wild-type corneas of the same age. Moreover, because the height-to-width at half-height ratio of the interfibrillar reflection from 2-month-old mutant corneas was also noticeably reduced (Table 2), it seems unlikely that a proper fibrillar arrangement is attained in the weeks after eye opening (i.e., by 2 months of age) and subsequently lost. Rather, collagen in the corneas of lumican-null mice appears to be in a state of disarray from early in life. This meshes with the finding by electron microscopy of a disorganized lamellar architecture in the corneas of lumican-deficient mice of ages similar to those studied here.[17] It should be noted, however, that previous electron microscopic work[17] has documented different amounts of disorder depending on stromal depth, of which more later.

What, then, are the implications for corneal transparency of the loss of order in the collagen array in lumican-null mice? Theory has it[35] that the fraction of light transmitted undeviated through the cornea $F(\lambda)$ is a function of the total scattering cross-section per fibril per unit length (σ), the number density of fibrils in the stroma (ρ), and the thickness of the tissue (t) and takes the form

$$F(\lambda) = e^{-\sigma\rho t}$$

Calculations of this sort are not trivial, particularly because the scattering cross-section per fibril length (σ) is itself a complex function of the wavelength of light, the diameters of the collagen fibrils, their mode of packing, and the ratio of the refractive index of the hydrated fibrils to the refractive index of the extrafibrillar matrix.[35] More extensive structural information from x-ray diffraction and electron microscopic investigations is required to fully model corneal transparency in lumican-deficient mice; however, we can predict that the altered fibril packing will modify σ and ρ and thus influence corneal transparency. Indeed, recent work with confocal microscopy through focusing (CMTF) has disclosed higher levels of backscatter in the corneas of lum^{tm1sc}/lum^{tm1sc} mice and has shown that that increased backscatter is a feature of younger (1–2-month-old) as well as older (4–5-month-old) animals.[17] Our results concur with this, in that they indicate that collagen disorganization is present early (2 months) as well as later (6 months) in life.

Although the collagen fibrils in the lumican-null corneas of both ages studied were more disordered than normal, we were able to obtain a value for the mean center-to-center collagen fibril spacings in the specimens that had been stored frozen (Tables 1, 2). Apart from one of the two 2-month-old wild-type corneas, the results were fairly consistent and indicated that the corneas of lumican-null mice, on average, had collagen fibrils that were a little more widely spaced than normal. It must be remembered, however, that we are quoting average values and when compared with the wild-type corneas, the mutant corneas, as indicated by the relative diffuseness of the interfibrillar reflections they generate, possessed rather more collagen fibrils that lay away from the quoted average. Also bear in mind that the values quoted are the interfibrillar Bragg spacings, values that do not take into account the mode of packing of the fibrils. If, as has often been done, a liquidlike packing of corneal collagen fibrils is envisaged, then the interfibrillar Bragg spacings should be multiplied by the factor 1.12 to give the actual center-to-center collagen fibril spacing.[31]

Previous x-ray diffraction studies of pathologic human corneas have shown collagen fibril spacing to be normal in keratoconus,[36] but compacted (in a nonuniform manner) in macular corneal dystrophy.[37] It is thus reasoned that keratoconic corneas are likely to be thin because the stroma contains less collagen than normal. Corneal thinness in macular corneal dystrophy, on the other hand, is judged to be caused mainly by the heterogeneous close packing of normal-diameter collagen fibrils. In the present study, the average interfibrillar spacings in the lum^{tm1sc}/lum^{tm1sc} and lum^{+}/lum^{+} corneas that had been stored frozen were not markedly different (Tables 1, 2), but the corneas of lumican-deficient mice are invariably in the region of 40% thinner than normal.[17] In view of this, we can reasonably conclude that the thinness of the mutant corneas is unlikely to be caused by the compaction of collagen fibrils. The most persuasive explanation is that there are simply fewer collagen fibrils in the mutant corneas. With this in mind, we point out the recent suggestion that lumican-null corneas are thin because of restricted collagen biosynthesis or because of a smaller pool of keratocytes.[17] This remains to be seen, although, if true, it would fit with our reasoning.

A prevailing theme of prior investigations into lum^{tm1sc}/lum^{tm1sc} corneas has been that it is the posterior stroma that is chiefly affected. Specifically, relatively more backscattered light is detected in deeper regions of the stroma, more lamellar disruption is reported there, collagen fibrils as a whole are a few percentage points larger than normal there, and more large and irregular fibrils abound.[17] Most of this information is acquired from electron microscopy. The x-ray reflections described herein were formed by a contribution to scattering from all collagen fibrils in a volume of the cornea through which the x-ray beam passes—in this case a volume that measured 1.5 × 1.0 mm × corneal thickness. This is an immense number of fibrils (of the order of 10^8), and our data thus provide highly representative average values for various stromal structures. The x-ray data also give a measure of these structures in a hydrated state. However, precisely because the x-ray beam passes through the whole cornea in these experiments, we were unable to identify the location with respect to depth of the structural alterations that we found. That said, the x-ray diffraction data are readily reconcilable with the results of the electron microscopic study of the lumican-null corneas, in that the interfibrillar reflection is "smeared out" because of fibrillar disorganization in the stromal matrix—a disorganization that electron microscopy has identified to be mostly in the posterior stroma.[17]

The first subsidiary x-ray reflection denoted by the elevated x-ray intensity around position $Q = 0.045\ nm^{-1}$ in Figures 2 and 3 is referred to as the fibril transform, and its position enables measurement of the average diameter of collagen fibrils throughout the whole tissue thickness. We did this in the 2-month-old and 6-month-old wild-type corneas that had been stored frozen (Tables 1, 2) and found that the value of approximately 35 nm was in the predicted range for hydrated mammalian corneas.[33] In stark contrast to the x-ray diffraction patterns from the corneas of wild-type mice, those from the corneas of lumican-null mutants did not possess a clear and consistently measurable fibril transform (Figs. 2, 3). This means that whereas collagen fibrils in normal corneas tend to be of a uniform diameter, those in the corneas of young and old lumican-deficient mice exhibit a clear variation is size. The electron microscopy concurs with this and further locates most large-diameter collagen fibrils in localized regions, in the deeper stromal layers.[17]

Regarding the possible mechanisms involved in the formation of larger than normal collagen fibrils, it is notable that, in vitro, lumican retards collagen fibrillogenesis and results in the formation of smaller fibrils.[38] In mice, we point out that higher levels of lumican are usually found in the posterior stroma,[17] and thus its absence is perhaps most strongly felt there, resulting in more large fibrils in that region of the tissue.[17] The picture regarding the influence of small leucine-rich proteoglycans in relation to the size of collagen fibrils in the corneal stroma is not yet fully resolved, however. For example, decorin, like lumican, retards collagen fibrillogenesis in vitro and results in the formation of smaller fibrils.[38] Nevertheless, initial reports show that gene-targeted decorin-null mice exhibit no apparent corneal abnormalities on electron microscopy.[39]

Work with transgenic models such as this can shed light on the pathologic mechanisms at play in human corneal disease. For example, in the inherited condition, macular corneal dystrophy, corneal clouding, and collagen ultrastructural abnormalities possibly caused by keratan sulfate proteoglycan deficiencies, are present, just as they are in the lumican-null mice.[9,10,15–17] However, there are key clinical, ultrastructural, and biochemical differences between the known types of macular corneal dystrophy and the lum^{tm1sc}/lum^{tm1sc} mouse investigated in this study. For example, unlike the lumican-null corneal phenotype in which corneal opacification is predominantly central with a peripheral clear zone, corneal clouding in macular corneal dystrophy extends to the limbal area. Also, in vivo CMTF has indicated increased backscattering (opacity) that is restricted to the posterior stroma in the lumican-deficient mouse, whereas in macular corneal dystrophy the opacification is superficial initially and later extends throughout the stroma. At the ultrastructural level, lumican-null corneas possess thicker than normal collagen fibrils and show a general lamellar disorganization in the posterior stroma that coincides well with the zone of increased backscattering.[17] These ultrastructural abnormalities are similar in some respects to those seen in macular corneal dystrophy, where an irregular pattern of collagen fibril packing has been reported,[40] along with some larger than normal collagen fibril diameters.[41,42]

Unlike the lumican-null cornea, however, a previous x-ray diffraction study on macular corneal dystrophy provided evidence for a heterogeneous, closer than normal interfibrillar spacing that was considered to be the underlying cause for the thin cornea.[37]Another difference between macular corneal dystrophy and the lumican deficient model in the present study is the reason for the absence of sulfated lumican. In the mutant mouse the lumican core protein, the major keratan sulfate–bearing core protein, is absent, and an assessment of total keratan sulfate content of whole eyes has indicated a 25% reduction in this molecule. In macular corneal dystrophy, on the other hand, mutations in a new carbohydrate sulfotransferase gene (*CHST6*)[43,44] and reduced enzyme activity[45] have been identified as the underlying cause of the poorly sulfated keratan sulfate proteoglycans.

Currently, experiments using transgenic technology aligned with a number of structural and biochemical tools are beginning to further enhance our understanding of corneal structure and function with regard to proteoglycans—for example, one form of the inherited condition cornea plana is now known to be caused by mutations in the gene that encodes keratocan, a small, leucine-rich proteoglycan that, similar to lumican, bears keratan sulfate side chains.[46] For a fuller understanding of the pathogenesis of macular corneal dystrophy we await the development of a transgenic model of this disease.

It is widely accepted that if the physical requirements for corneal transparency are to be met, then the collagen fibrils that make up the corneal stroma must be of approximately the same diameter and configured in a fairly regular array. The spatial arrangement of stromal collagen in the corneas of lumican-deficient mice was in disarray, and there was a significant variation in the diameter of the hydrated collagen fibrils that is not ordinarily seen in normal corneas. These abnormalities, which are present from an early age, probably contribute to the reduced transparency in the corneas of lumican-null mice.

Acknowledgments

The authors thank Gunter Grossmann for help at the synchrotron and Richard Newton for assistance with data analysis.

References

1. Hassell JR, Cintron C, Kublin C, Newsome DA. Proteoglycan changes during restoration of transparency in corneal scars. *Arch Biochem Biophys.* 1983;222:362–369.
2. Funderburgh JL, Cintron C, Covington HI, Conrad GW. Immunoanalysis of keratan sulfate proteoglycan from corneal scars. *Invest Ophthalmol Vis Sci.* 1988;29:1116–1124.
3. Cintron C, Covington HI, Kublin CL. Morphologic analyses of proteoglycans in corneal scars. *Invest Ophthalmol Vis Sci.* 1990; 31:1789–1797.
4. Cintron C, Gregory JD, Dalme SP, Kublin CL. Biochemical analyses of proteoglycans in rabbit corneal scars. *Invest Ophthalmol Vis Sci.* 1990;31:1975–1981.
5. Cornuet PK, Blochberger TC, Hassell JR. Molecular polymorphism of lumican during corneal development. *Invest Ophthalmol Vis Sci.* 1994;35:870–877.
6. Cai CX, Gibney E, Gordon MK, Marchant JK, Birk DE, Linsenmayer TF. Characterization and developmental regulation of avian corneal β-1,4-galactosyltransferase mRNA. *Exp Eye Res.* 1996;63:193–200.
7. Dunlevy JR, Beales MP, Berryhill BL, Cornuet PK, Hassell JR. Expression of the keratan sulfate proteoglycans lumican, keratocan and osteoglycin/mimecan during chick corneal development. *Exp Eye Res.* 2000;70:349–362.
8. Ying S, Shiraishi A, Kao CW-C, et al. Characterization and expression of the mouse lumican gene. *J Biol Chem.* 1997;272:30306–30313.
9. Hassell JR, Newsome DA, Krachmer JH, Rodrigues MM. Macular corneal dystrophy: failure to synthesize a mature keratan sulfate proteoglycan. *Proc Natl Acad Sci USA.* 1980;77:3705–3709.
10. Klintworth GK, Oshima E, Al-Rajhi A, Al-Saif A, Thonar EJ-MA, Karcioglu ZA. Macular corneal dystrophy in Saudi Arabia: a study of 56 cases and recognition of a new immunophenotype. *Am J Ophthalmol.* 1997;124:9–18.
11. Blochberger TC, Vergnes J-P, Hempel J, Hassell JR. cDNA to chick lumican (corneal keratan sulfate proteoglycan) reveals homology to the small interstitial proteoglycan gene family and expression in muscle and intestine. *J Biol Chem.* 1992;267:347–352.

12. Corpuz LM, Funderburgh JL, Funderburgh ML, Bottomley GS, Prakash S, Conrad GW. Molecular cloning and tissue distribution of keratocan: bovine corneal keratan sulfate proteoglycan 37A. *J Biol Chem.* 1996;271:9759–9763.
13. Liu C-Y, Shiraishi A, Kao CW-C, et al. The cloning of mouse keratocan cDNA and genomic DNA and the characterization of its expression during eye development. *J Biol Chem.* 1998;273: 22584–22588.
14. Funderburgh JL, Corpuz LM, Roth MR, Funderburgh ML, Tasheva ES, Conrad GW. Mimecan, the 25-kDa corneal keratan sulfate proteoglycan, is a product of the gene producing osteoglycin. *J Biol Chem.* 1997;272:28089–28095.
15. Chakravarti S, Magnuson T, Lass JH, Jepsen KJ, LaMantia C, Carroll H. Lumican regulates collagen fibril assembly: skin fragility and corneal opacity in the absence of lumican. *J Cell Biol.* 1998;141: 1277–1286.
16. Saika S, Shirashi A, Saika S, et al. Role of lumican in the corneal epithelium during wound healing. *J Biol Chem.* 2000;275:2607–2612.
17. Chakravarti S, Petroll WM, Hassell JR, et al. Corneal opacity in lumican-null mice: defects in collagen fibril structure and packing in the posterior stroma. *Invest Ophthalmol Vis Sci.* 2000;41:3365–3373.
18. Borcherding MS, Blacik LJ, Sittig RA, Bizzell JU, Breen M, Weinstein HG. Proteoglycans and collagen fibre organization in human corneoscleral tissue. *Exp Eye Res.* 1975;21:59–70.
19. Maurice DM. The structure and transparency of the corneal stroma. *J Physiol.* 1957;136:263–286.
20. Hart RW, Farrell RA. Light scattering in the cornea. *J Opt Soc Am.* 1969;59:766–774.
21. Benedek GB. Theory and transparency of the eye. *Appl Opt.* 1971; 10:459–473.
22. Freund DE, McCally RL, Farrell RA, Cristol SM, L'Hernault NL, Edelhauser HF. Ultrastructure in anterior and posterior stroma of perfused human and rabbit corneas: relation to transparency. *Invest Ophthalmol Vis Sci.* 1995;36:1508–1523.
23. Meek KM, Quantock AJ. The use of x-ray scattering techniques to determine corneal ultrastructure. *Prog Retinal Eye Res.* 2001;20: 95–137.
24. Daxer A, Fratzl P. Collagen fibril orientation in the human corneal stroma and its implications in keratoconus. *Invest Ophthalmol Vis Sci.* 1997;38:121–129.
25. Leonard DW, Meek KM. Estimation of the refractive indices of collagen fibrils and ground substance of the corneal stroma using data from x-ray diffraction. *Biophys J.* 1997;72:1382–1387.
26. Quantock AJ, Kinoshita S, Capel MS, Schanzlin DJ. A synchrotron x-ray diffraction study of developing chick corneas. *Biophys J.* 1998;74:995–998.
27. Daxer A, Misof K, Grabner B, Ettl A, Fratzl P. Collagen fibrils in the human corneal stroma: structure and ageing. *Invest Ophthalmol Vis Sci.* 1998;39:644–648.
28. Newton RH, Meek KM. Circum-corneal annulus of collagen fibrils in the human limbus. *Invest Ophthalmol Vis Sci.* 1998;39:1125–1134.
29. Connon CJ, Meek KM, Newton RH, Kenney MC, Alba SA, Karageozian H. Hyaluronidase treatment, collagen fibril packing, and normal transparency in rabbit corneas. *J Refract Surg.* 2000;16: 448–455.
30. Fullwood NJ, Meek KM. A synchrotron x-ray study of the changes occurring in the corneal stroma during processing for electron microscopy. *J Microsc.* 1992;169:53–60.
31. Worthington CR, Inouye H. X-ray diffraction study of the cornea. *Int J Biol Macromol.* 1985;7:2–8.
32. Vainshtein BK. *Diffraction of X-Rays by Chain Molecules*. Amsterdam: Elsevier; 1966.
33. Meek KM, Leonard DW. The ultrastructure of the corneal stroma: a comparative study. *Biophys J.* 1993;64:273–280.
34. Rawe IM, Meek KM, Leonard DW, Takahashi T, Cintron C. Structure of corneal scar tissue: an x-ray diffraction study. *Biophys J.* 1994;67:1743–1748.
35. Farrell RA. Corneal transparency. In: Albert DM, Jacobiec SA, eds. *Principles and Practice of Ophthalmology.* Philadelphia: Saunders; 1994.
36. Fullwood NJ, Tuft SJ, Malik NS, Meek KM, Ridgway AEA, Harrison RJ. Synchrotron X-ray diffraction studies of keratoconus corneal stroma. *Invest Ophthalmol Vis Sci.* 1992;33:1734–1741.
37. Quantock AJ, Meek KM, Ridgway AEA, Bron AJ, Thonar EJ-MA. Macular corneal dystrophy: reduction in both corneal thickness and collagen interfibrillar spacing. *Curr Eye Res.* 1990;9:393–398.
38. Rada J, Cornuet PK, Hassell JR. Regulation of corneal collagen fibrillogenesis in vitro by corneal proteoglycan (lumican and decorin) core proteins. *Exp Eye Res.* 1993;56:635–648.
39. Danielson KG, Baribault H, Holmes DF, Graham H, Kadler KE, Iozzo RV. Targeted disruption of decorin leads to abnormal collagen fibril morphology and skin fragility. *J Cell Biol.* 1997;136:729–743.
40. Meek KM, Quantock AJ, Elliott GF, et al. Macular corneal dystrophy: the macromolecular structure of the stroma observed using electron microscopy and synchrotron x-ray diffraction. *Exp Eye Res.* 1989;49:941–958.
41. Quantock AJ, Meek KM, Thonar EJ-MA, Assil KK. Synchrotron x-ray diffraction in atypical macular dystrophy. *Eye.* 1993;7:779–784.
42. Quantock AJ, Fullwood NJ, Thonar EJ-MA, et al. Macular corneal dystrophy type II: multiple studies on a cornea with low levels of sulfated keratan sulfate. *Eye.* 1997;11:57–67.
43. Akama TO, Nishida K, Nakayama J, et al. Macular corneal dystrophy type I and type II are caused by distinct mutations in a new sulphotransferase gene. *Nat Genet.* 2000;26:237–241.
44. Lui N-P, Sew-Knight S, Rayner M, et al. Mutations in corneal carbohydrate sulphotransferase 6 gene (CHST6) cause macular corneal dystrophy in Iceland. *Mol Vis.* 2000;6:261–264.
45. Hasegawa N, Torii T, Kato T, et al. Decreased GlcNAc 6-O-sulphotransferase activity in the cornea with macular corneal dystrophy. *Invest Ophthalmol Vis Sci.* 2000;41:3670–3677.
46. Pellegata NS, Dieguez-Lucena JL, Joensuu T, et al. Mutations in KERA, encoding keratocan, cause cornea plana. *Nat Genet.* 2000; 25:91–95.